科学通报 2022 年 第 67 卷 第 20 期: 2423 ~ 2430
庆祝北京师范大学建校120周年暨化学学科创立110周年专辑 论 文
《中国科学》杂志社 SCIENCE CHINA PRESS

用于高效电催化析氧反应的锰掺杂镍铁双金属氢氧化物催化剂

孙泽民[1,2], 刘宇慧[1], 丁大杰[1], 罗澜柯[1], 李志杰[1], 袁萌伟[1], 孙根班[1,2*]

1. 北京师范大学化学学院, 能量转换与存储材料北京市重点实验室, 北京 100875;
2. 北京师范大学珠海校区自然科学高等研究院, 先进材料中心, 珠海 519087
* 联系人, E-mail: gbsun@bnu.edu.cn

2021-12-19 收稿, 2022-02-17 修回, 2022-03-22 接受, 2022-03-25 网络版发表
国家自然科学基金(21771024)资助

摘要 随着国内能源需求不断增加以及温室气体排放持续增长, 寻求高效、清洁、可持续的能源成为目前亟待解决的问题. 廉价、高效和稳定的氧析出反应(oxygen evolution reaction, OER)催化剂在电解水制氢领域具有广泛的应用前景. 镍铁层状双金属氢氧化物(NiFe-layered double hydroxides, NiFe-LDHs)被认为是一种潜在、理想的析氧反应电催化剂. 然而, 对于NiFe-LDHs层板, 普遍认为其边缘金属位点相较于内部金属位点具有更高的催化活性, 这就导致其层板内部的金属位点无法充分利用, 降低对OER反应的催化效率. 因此, 为了充分提升NiFe-LDHs的层板利用率, 本研究将具有变价特征的锰离子引入NiFe-LDHs层板(Mn doped NiFe-layered double hydroxides, Mn-NiFe-LDHs)中, 利用锰离子的变价特征, 充分提升层板载流子迁移率, 促进层板内电子转移, 同时, 由于锰离子的电负性特征, 部分电子将从镍位点附近转移到锰位点的周围, 导致镍位点表现出缺电子特征, 从而作为"电子饥饿"位点, 提升层板整体对于具有富电子含氧官能团的捕获, 进而有效地增强OER催化活性. 催化反应结果表明, Mn-NiFe-LDHs电极在电流密度10 mA/cm^{2}时表现出过电位仅为332 mV, 低于初始NiFe-LDHs的384 mV. 锰离子的合理掺杂有效地调整Ni^{2+}位点活性, 增强其电催化活性, 并为更进一步地阐明掺杂对LDHs层板活性的影响提供了实验事实支持.

关键词 电化学, 掺杂调控, 镍铁水滑石, 析氧反应

氢能具有来源广、热值高、清洁、可再生等诸多优势, 被认为是一种理想的二次能源[1,2]. 在"碳达峰、碳中和"("双碳")的背景下, 发展氢能已成为世界各国的战略部署. 近年来, 我国政府也提出"双碳"目标. 推进氢能产业的快速发展已成为时代发展的关键需求. 通过利用可再生能源转化为电能, 进一步通过电能实现电解水制氢, 目前被认为是最为安全、绿色的制氢途径[3,4]. 然而, 在实际的电解水制氢过程中, 存在反应过电位高、电能转换效率低等问题, 严重制约了电解水制氢的成本, 限制了其商业化运用的进程[5,6]. 电解水过程中, 阴、阳两极电极分别发生析氢反应(hydrogen evolution reaction, HER)和析氧反应(oxygen evolution reaction, OER). 与二电子反应的HER过程相比, 四电子的OER过程需要更高的过电位[7,8]. 因此, 四电子OER过程成为反应的决速步. 为了实现高效率、低能耗的电解水制氢过程, 亟需廉价、高效且稳定的OER催化剂[7~12]. 目前, 寻找高效、低成本的OER催化剂仍是电解水反应的"圣杯". 在众多非贵金属催化剂中, 镍

引用格式: 孙泽民, 刘宇慧, 丁大杰, 等. 用于高效电催化析氧反应的锰掺杂镍铁双金属氢氧化物催化剂. 科学通报, 2022, 67: 2423–2430
Sun Z M, Liu Y H, Ding D J, et al. Manganese-doped nickel-iron bimetallic hydroxide catalyst for efficient electrocatalytic oxygen evolution reaction (in Chinese). Chin Sci Bull, 2022, 67: 2423–2430, doi: 10.1360/TB-2021-1323

铁层状双金属氢氧化物(NiFe-layered double hydroxides, NiFe-LDHs)由于其原料成本低、结构可调以及高比表面积和高活性位点暴露率的特点，被认为是碱性条件下理想的OER电催化剂，受到研究人员的广泛关注. 但是，与边缘金属活性位点相比，层板内的金属位点是惰性的, 这导致了对层板金属位点的利用不足.

为了解决上述问题, 近几十年来, 科研人员在NiFe-LDHs微观结构调控的基础上，对NiFe-LDHs进行改性，提升其在OER过程中的催化活性和稳定性[13,14]. 通过对层板进行异质元素掺杂被认为是一种调节催化剂电子结构和电化学活性的有效方法. 金属离子掺杂(Cr、Cu、V等)可以实现镍金属活性位点的电子结构优化，降低反应过电位，提升催化效率[15~21]. 然而，传统的过渡金属(Cr、V、Cu等)具有较高的生物毒性，限制了其工业化推广. 具有丰富变价特征的Mn($Mn^{2+}\rightleftharpoons Mn^{3+}\rightleftharpoons Mn^{4+}$)具有潜在调控层板电荷特性的作用[22,23].

本研究通过水热法，在碳纸表面生长具有高原子暴露率的NiFe-LDHs和Mn-NiFe-LDHs纳米阵列，提升LDHs在OER过程中的电子输运能力和气体扩散动力学. 通过锰离子掺杂有效地调控层板结构, 优化活性中心的电子结构, 充分利用掺杂离子的诱导作用, 可以产生新的耦合作用，在10 mA/cm^{2}的电流密度下，过电位降低了52 mV, 其有效地降低催化反应的过电位，提升催化活性和稳定性.

1 实验

(ⅰ) 材料. $MnSO_4\cdot 6H_2O$(分析纯)、$CuSO_4\cdot 5H_2O$(分析纯)、$Fe(NO_3)_3\cdot 9H_2O$(分析纯)和$Ni(NO_3)_2\cdot 6H_2O$(分析纯)来源于韦斯(北京)实验用品有限公司; 脲(分析纯)和CH_3CH_2OH(分析纯)购自北京化工厂；亲水碳纸(HCP020)采购于常州优特科新能源科技；铂片电极(10 mm×10 mm×1 mm)和Hg/HgO电极(电解液为1.0 mol/L KOH溶液)购自武汉高仕睿联科技有限公司.

(ⅱ) 仪器. X射线粉末衍射仪(X-ray diffraction, XRD, XPertPROMPD, PANalytical公司, 荷兰)和X射线光电子能谱(X-ray photoelectron spectroscopy, XPS, ESCALAB 250Xi, FEI公司, 美国)进行结构表征; 扫描电子显微镜(scanning electron microscope, SEM, SU-0810，日立公司，日本)和透射电子显微镜(transmission electron microscope, TEM, FEI G2 F20, FEI公司, 美国)进行微观形貌表征；电化学工作站(CHI440C，上海辰华)和阻抗分析仪(Zennium IM6，Zahner，德国)进行电化学性能表征；真空干燥箱(DZF-6020，一恒科学仪器有限公司，中国)和分析天平(EL 104, 北京赛多利仪器系统有限公司, 中国)应于催化剂的合成和制备.

(ⅲ) NiFe-LDHs的制备. 称取6 mmol $Ni(NO_3)_2\cdot 6H_2O$、2 mmol $Fe(NO_3)_3\cdot 9H_2O$和20 mmol脲经超声充分溶解于40 mL去离子水中得澄清分散液, 加入去离子水配成80 mL混合溶液转移入水热反应釜，于烘箱中140°C反应6 h，自然冷却，将沉淀依次用去离子水、无水乙醇洗涤3次并离心, 在100°C干燥6 h.

(ⅳ) 锰离子掺杂NiFe-LDHs的制备(Mn-NiFe-LDHs). 称取6 mmol $Ni(NO_3)_2\cdot 6H_2O$、2 mmol $Fe(NO_3)_3\cdot 9H_2O$、1 mmol $MnSO_4\cdot 6H_2O$和20 mmol脲经超声充分溶解于40 mL去离子水中得澄清分散液, 加入去离子水配成80 mL混合溶液转移入水热反应釜，于烘箱中140°C反应6 h，自然冷却，将沉淀依次用去离子水、无水乙醇洗涤3次并离心，在100°C干燥6 h，得到Mn-NiFe-LDHs.

(ⅴ) NiFe-LDHs和Mn-NiFe-LDHs碳纸样品的制备. 掺杂量及比例与上述一致，在配成的80 mL混合溶液中加入蒸馏水超声洗涤3次后的亲水碳纸，共同水热140°C反应6 h，自然冷却. 取出碳纸用蒸馏水、乙醇洗涤3次, 得到NiFe-LDHs和Mn-NiFe-LDHs的碳纸样品.

(ⅵ) 电化学性能测试. 在标准的三电极系统中(石墨作为对电极, Hg/HgO电极作为参比电极, NiFe-LDHs作为工作电极)，使用Zennium IM6站电化学分析仪进行电化学测量. 利用线性扫描伏安(linear sweep voltammetry，LSV)曲线测试了在1.0 mol/L KOH中OER的性能, 扫描速率为5 mV/s. 根据下式将电势转换为可逆氢电极(RHE)：$E_{RHE}=E_{Hg/HgO}+0.098+0.0591\times pH$，由$\eta=E_{RHE}-1.23$ V计算OER的过电位(η). 在0.01 Hz~100 kHz频率范围内、1.0 mol/L KOH溶液中, 用振幅为5 mV的交流电压测量电化学阻抗谱(electrochemical impedance spectrum, EIS) .

2 结果与讨论

2.1 结构表征

以脲为碱源，采用水热共沉淀法成功制备了NiFe-LDHs和Mn-NiFe-LDHs. 对其结构进行表征, 通过XRD谱图确定合成样品的结构(图1(a)). XRD测试结果表明，其与α-$Ni(OH)_2$(JCPDS No. 38-0715)相吻合，在11.3°、22.7°、33.5°、34.4°、38.8°、46.0°、60.0°、61.3°分别

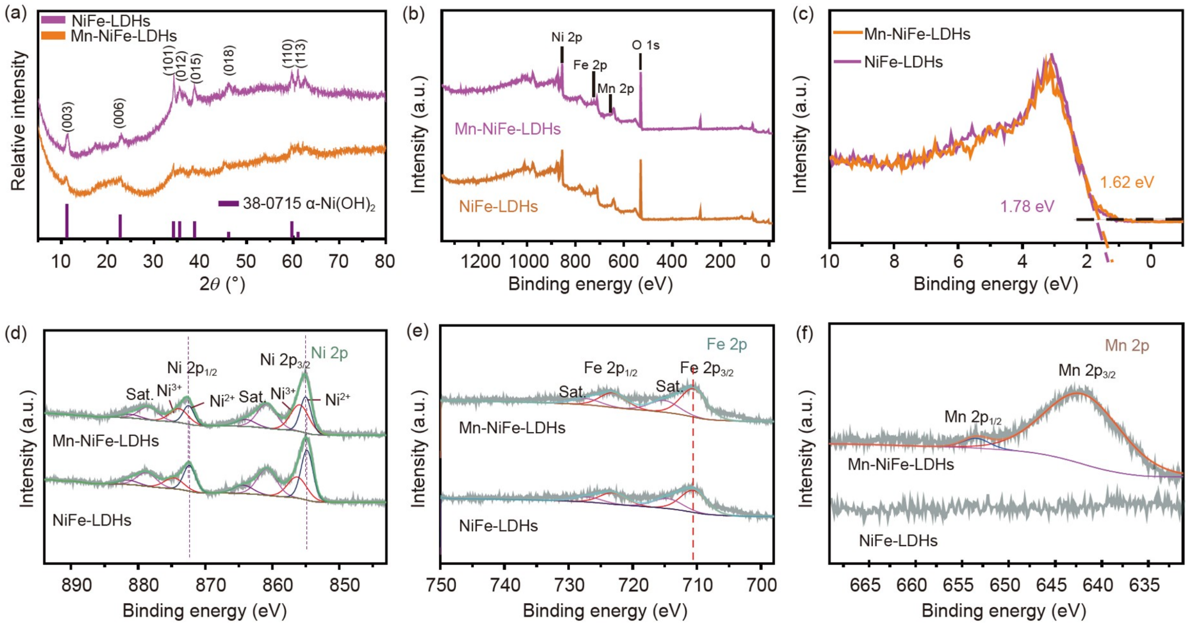

图 1 NiFe-LDHs和Mn-NiFe-LDHs结构表征. (a) XRD; (b) XPS; (c) 价带谱; Ni 2p(d)、Fe 2p(e)和Mn 2p(f)的高分辨XPS谱

Figure 1 The structure characterization of NiFe-LDHs and Mn-NiFe-LDHs. (a) XRD; (b) XPS; (c) valence band spectra; high-resolution XPS scans of Ni 2p (d), Fe 2p (e) and Mn 2p (f)

出现(003)、(006)、(101)、(012)、(015)、(018)、(110)、(113)衍射峰，与文献[15,24]报道的NiFe-LDHs衍射峰一致．与NiFe-LDHs相比，由于锰离子的引入，Mn-NiFe-LDHs的衍射峰强度降低，半峰宽变宽，这暗示着锰离子的引入有效地降低了NiFe-LDHs层板的结晶度．同时，锰离子的引入使得其层板峰发生位移，其具体表现在: 层板峰向小角度移动．通过ICP-AES确定催化剂NiFe-LDHs和Mn-NiFe-LDHs的负载量约为2.0 mg/cm^2，其中对于NiFe-LDHs，Ni:Fe=2.98:1.12，对于Mn-NiFe-LDHs，Mn:Ni:Fe=0.46:2.95:1.13，金属元素的摩尔比与投料中金属离子摩尔比相近．为了进一步评估引入锰元素对NiFe-LDHs层板电子结构的影响，通过XPS分析掺杂前后不同元素电子结构的变化. 根据XPS总谱结果(图1(b))，Mn元素成功地引入到LDHs层板中．如图1(c)所示，对NiFe-LDHs以及Mn-NiFe-LDHs的价带进行测试，可以看到Mn-NiFe-LDHs的价带比NiFe-LDHs更接近费米能，锰元素的引入有效地优化了NiFe-LDHs层板的能带结构，进而增强了其电催化过程中的电子传输性能. Ni和Fe的XPS精细谱如图1(c), (d)所示．对于Ni$_{2p}$存在两组峰，分别属于Ni^{2+}和Ni^{3+}. 855.5和873.4 eV处的两个峰对应Ni^{2+} 2p$_{1/2}$和2p$_{3/2}$, 857.4和875.5 eV处的两个峰对应Ni^{3+} 2p$_{1/2}$和2p$_{3/2}$．与NiFe-LDHs相比，Mn-NiFe-LDHs中Ni峰的位置向高结合能方向移动，暗示着Ni^{3+}组分由初始的32%增加至61%，Ni^{3+}组分含量明显增强. 根据文献[25,26]报道，随着Ni^{3+}配比的增加，可以有效地促进OER催化动力学增强．对于Fe 2p(图1(e))，由于Mn与Fe的电负性相近，锰的引入对Fe周围的电荷分布影响不大，存在两个典型的Fe^{3+}特征峰．为了精确证明和确认锰的存在，测量了Mn 2p的XPS谱图，通过对比，进一步证明锰离子被成功地引入NiFe-LDHs的层板(图1(f)). 结果表明，锰离子被成功地引入NiFe-LDHs层板中，成功诱导和优化了电子态与能带，提升了层板的金属位点的有效活性.

2.2 形貌表征

为了避免黏结剂的干扰，提高电子传输性能，将NiFe-LDHs和Mn-NiFe-LDHs通过水热法，原位生长在碳纸上．通过SEM进行表征，如图2(a), (b)所示，NiFe-LDHs和Mn-NiFe-LDHs均以纳米片阵列的形式均匀生长在碳纸表面，并且锰离子的引入未对其结构造成明显的影响．进一步利用TEM和选区电子衍射(selected area electron diffraction, SAED)分析了催化剂微观结构．从TEM可以看出，它们都表现出超薄纳米片形貌(图2(c1), (d1))．利用SAED对其精细结构进行分析，如图2(c1)插图所示，NiFe-LDHs结晶性良好，具有良好的六方结构. 随着锰离子的引入，层板的结晶度明显降低，

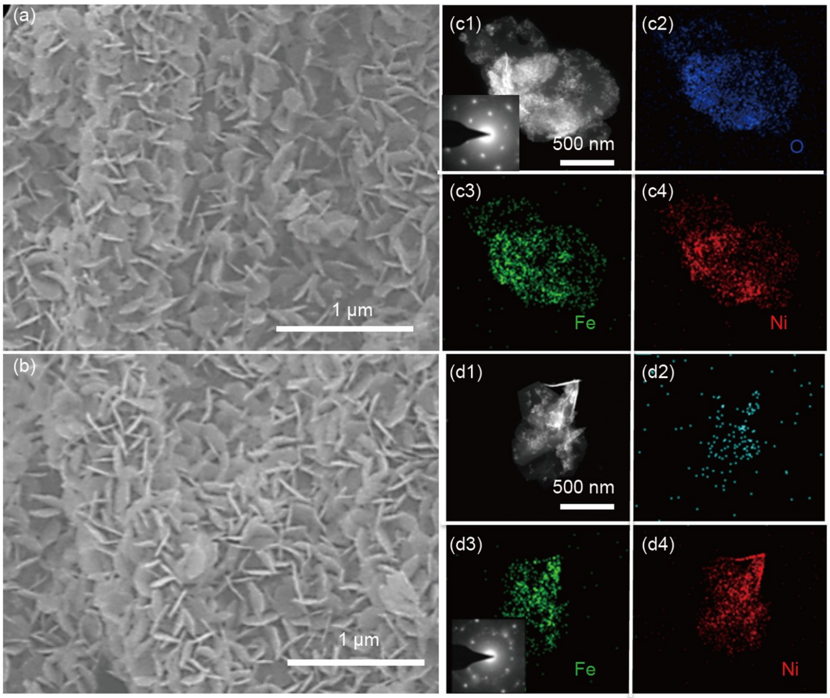

图 2 NiFe-LDHs和Mn-NiFe-LDHs形貌表征. NiFe-LDHs(a)和Mn-NiFe-LDHs(b)的SEM图; (c1) NiFe-LDHs的TEM, 插图为SAED图, (c2)~(c4)分别为O、Fe、Ni的元素分布图; (d1) Mn-NiFe-LDHs的TEM, (d2)~(d4) 分别为Mn、Fe、Ni的元素分布图; (d3) 插图为SAED图

Figure 2 The morphology characterization of NiFe-LDHs and Mn-NiFe-LDHs. The SEM of NiFe-LDHs (a) and Mn-NiFe-LDHs (b); (c1) the TEM (the inset is SAED pattern) and the energy dispersive spectroscopy (EDS) mapping of O (c2), Fe (c3) and Ni (c4) for NiFe-LDHs; (d1) the TEM and the EDS mapping of Mn (d2), Fe (d3) and Ni (d4) for Mn-NiFe-LDHs; the inset in (d3) is SAED pattern

如图2(d3)插图所示, 其无序性增加, 这与上述XRD结果一致. 对应的元素分布结果(图3(c2)~(c4))表明, 元素镍、铁、氧均匀分布. 与NiFe-LDHs相比, Mn元素均匀分布在Mn-NiFe-LDHs(图3(d2)~(d4))层板上, 进一步证明锰离子的成功引入.

2.3 催化性能表征

为了进一步验证其构效关系, 对NiFe-LDHs和Mn-NiFe-LDHs进行了一系列的电化学性能测试. 所有测试均在1.0 mol/L KOH电解液中采用三电极系统进行. NiFe-LDHs、Mn-NiFe-LDHs以及碳纸LSV曲线如图3(a)所示, 碳纸几乎没有OER活性. 与NiFe-LDHs相比, Mn-NiFe-LDHs可以有效地提升OER活性, 降低催化反应的过电位. 不同电流密度下的过电位如图3(b)所示, Mn-NiFe-LDHs在1.0 mA/cm^{2}时的过电位仅为267 mV, 在10 mA/cm^{2}时, 仅为332 mV, 优于NiFe-LDHs(288 mV@1.0 mA/cm^{2}和374 mV@10mA/cm^2), 这表明锰离子的引入有效地增强NiFe-LDHs的OER活性, 如表1所示, 优于目前已报道的一些碱性OER电催化剂. 通过Tafel图和EIS对OER动力学进行了评估. 如图3(c)所示, Mn-NiFe-LDHs的Tafel斜率为75.8 mV/dec, 优于NiFe-LDHs(98.6 mV/dec), 表明锰离子的引入有效地提升了产氧速率和OER动力学. EIS阻抗谱的直径越小, 电催化剂的电荷转移电阻(R_{ct})越小. 对EIS阻抗谱进行等效电路模拟(图3(d), Mn-NiFe-LDHs具有较低的电荷转移电阻. Tafel斜率和EIS均表明Mn-NiFe-LDHs更有利于OER过程. 稳定性是研究催化活性的一个重要指标, 通过时间-电位测定实验评估催化剂的稳定性(图3(e)). Mn-NiFe-LDHs电极在恒电位1.6 V下的电流密度损失很小, 在70 h内表现出优异的长期耐久性.

2.4 催化机理分析

对Mn-NiFe-LDHs增强OER反应的机理进行了探究. 样品进行CV活化(图4), 存在两个明显的氧化还原峰, 这是由于具有变价特征的Mn元素在反应过程中发生不完全可逆循环, 存在两组Mn^{2+}⇌ Mn^{3+}⇌Mn^{4+}的氧化还原峰, 进一步表明变价锰离子可以促进催化活性. 这将对Ni元素价态产生影响, 进而实现对OER催化性

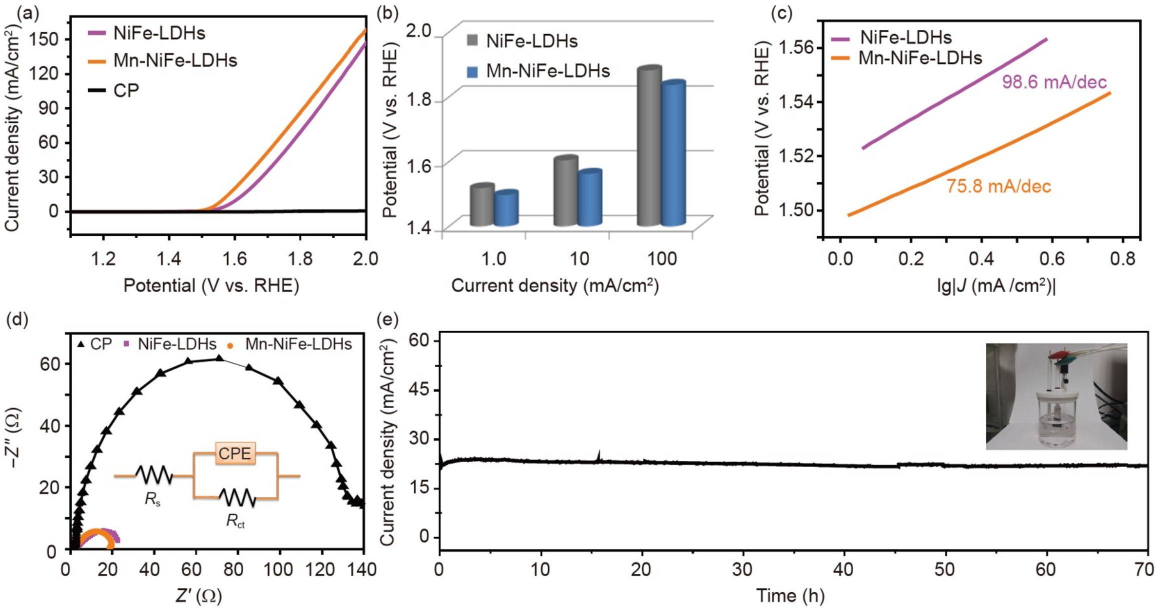

图 3 OER性能表征. (a) NiFe-LDHs、Mn-NiFe-LDHs和CP的极化曲线. (b) 1、10和100 mA/cm^{2}的过电位. (c) NiFe-LDHs和Mn-NiFe-LDHs的Tafel图. (d) NiFe-LDHs和Mn-NiFe-LDHs的Nyquist图, 插图为模拟电路图. (e) 在1.0 mol/L KOH电解质中1.6 V下的催化稳定性测试, 插图为OER测试装置图

Figure 3 The OER performance characterization. (a) Polarization curves of NiFe-LDHs, Mn-NiFe-LDHs and CP. (b) The overpotential at 1, 10 and 100 mA/cm^2. (c) Tafel plots of NiFe-LDHs and Mn-NiFe-LDHs. (d) Nyquist plots of NiFe-LDHs and Mn-NiFe-LDHs; the inset is an analog circuit diagram of Nyquist plots. (e) The long-term durability tests at 1.6 V in a 1.0 mol/L KOH electrolyte; the inset is an OER test device photograph

表 1 **Mn-NiFe-LDHs与其他OER电催化剂性能比较**

Table 1 Comparison of OER performance in alkaline for Mn-NiFe-LDHs with OER electrocatalysts

催化剂	j(mA/cm^2)	η(mV)	参考文献
Mn-NiFe-LDHs	10	332	本文
NiCo-LDHs	10	367	[27]
NiCo-LDHs纳米片	10	420	[28]
Co_3O_4	10	490	[29]
CoMn-LDHs	10	324	[30]
Co_3O_4	10	410	[31]
$ZnCo_2O_4$	10	390	[31]
ZnCo-LDHs	10	370	[32]
Co-NC/CNT/NF	10	354	[33]
Co–Zn/PNC/NF	10	348	[34]
3D-CNTA/NF	10	360	[35]

能的提升. 故此对Mn-NiFe-LDHs活化后的材料进行XPS表征(图5(a)~(c)). 结果发现, 在XPS图谱中Ni 2P轨道不断向高结合能方向移动, Mn 2p轨道向低结合能方向移动, 说明具有变价特征Mn元素的掺杂确实在反应过程中发生了不完全可逆的电化学活化, 导致了更多高活性的Ni^{3+}, 由此提升了层板的OER性能.

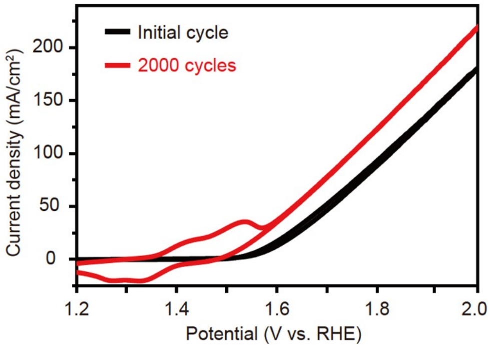

图 4 1.0 mol/L KOH条件下初始第1次和第2000次CV曲线

Figure 4 The CVs curve of the initial cycle and the 2000th cycles in 1.0 mol/L KOH

3 结论

综上所述, 本文开发了一种简单、高效的水热共沉淀法, 通过将催化剂原位生长在碳纸表面, 提升催化剂活性位点的暴露率. 同时, 锰元素成功地引入到NiFe-LDHs的晶格中, 有效地优化了NiFe-LDHs层板的能带结构, 进而增强了其层板的电子传输性能. 锰的引入使得Ni峰的位置向高结合能方向移动, 暗示着Ni^{3+}组分的含量明显增加, 有效地促进OER催化动力学. 锰的引入

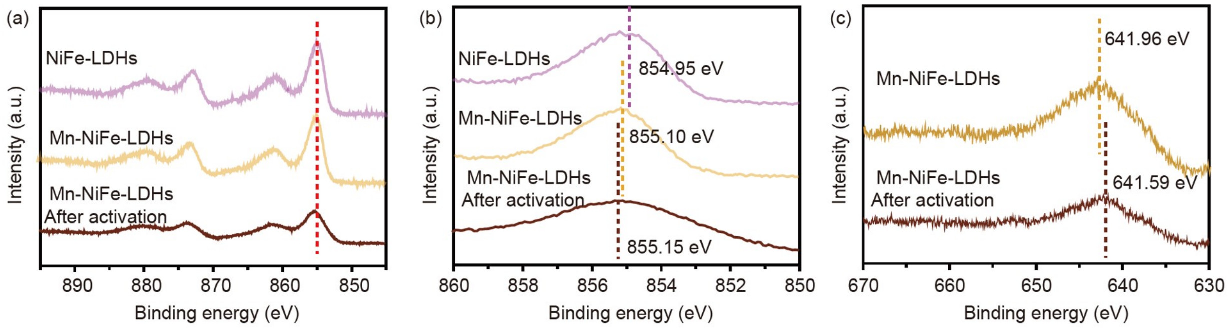

图 5 NiFe-LDHs、Mn-NiFe-LDHs和Mn-NiFe-LDHs活化后的XPS精细图谱. (a) Ni 2p; (b) (a)图中Ni 2p的放大图; (c) Mn 2p

Figure 5 The XPS of the NiFe-LDHs, Mn-NiFe-LDHs和Mn-NiFe-LDHs after activation. (a) Ni 2p; (b) the enlarged part of (a) for Ni 2p; (c) Mn 2p

提升了层板金属位点的有效活性，并有效地提升了NiFe-LDHs的OER性能．本研究将有助于拓宽电催化剂界面和纳米结构的合理设计，为催化剂的设计和研究提供借鉴价值.

参考文献

1 Hu C, Zhang L, Gong J. Recent progress made in the mechanism comprehension and design of electrocatalysts for alkaline water splitting. Energy Environ Sci, 2019, 12: 2620–2645

2 Sun H, Yan Z, Liu F, et al. Self-supported transition-metal-based electrocatalysts for hydrogen and oxygen evolution. Adv Mater, 2020, 32: 1806326

3 Yuan Y, Lei A. Electrochemical oxidative cross-coupling with hydrogen evolution reactions. Acc Chem Res, 2019, 52: 3309–3324

4 Yang R, Zhou Y, Xing Y, et al. Synergistic coupling of CoFe-LDH arrays with NiFe-LDH nanosheet for highly efficient overall water splitting in alkaline media. Appl Catal B-Environ, 2019, 253: 131–139

5 Suryanto B H R, Wang Y, Hocking R K, et al. Overall electrochemical splitting of water at the heterogeneous interface of nickel and iron oxide. Nat Commun, 2019, 10: 5599

6 Wang H F, Chen L, Pang H, et al. MOF-derived electrocatalysts for oxygen reduction, oxygen evolution and hydrogen evolution reactions. Chem Soc Rev, 2020, 49: 1414–1448

7 Bai L, Hsu C S, Alexander D T L, et al. A cobalt-iron double-atom catalyst for the oxygen evolution reaction. J Am Chem Soc, 2019, 141: 14190–14199

8 Song J, Wei C, Huang Z F, et al. A review on fundamentals for designing oxygen evolution electrocatalysts. Chem Soc Rev, 2020, 49: 2196–2214

9 Sun Z, Yuan M, Yang H, et al. Vacancy-defects turn off conjugated π bond shield activated catalytic molecular adsorption process. Appl Surf Sci, 2021, 543: 148790

10 Sun Z, Wang D, Lin L, et al. Ultrathin hexagonal boron nitride as a van der Waals' force initiator activated graphene for engineering efficient non-metal electrocatalysts of Li-CO_2 battery. Nano Res, 2022, 15: 1171–1177

11 Sun Z, Wang X, Yuan M, et al. "Lewis Base-Hungry" amorphous-crystalline nickel borate-nickel sulfide heterostructures by *in situ* structural engineering as effective bifunctional electrocatalysts toward overall water splitting. ACS Appl Mater Interfaces, 2020, 12: 23896–23903

12 Sun Z, Yuan M, Lin L, et al. Perovskite $La_{0.5}Sr_{0.5}CoO_{3-\delta}$ grown on $Ti_3C_2T_x$MXene nanosheets as bifunctional efficient hybrid catalysts for Li-oxygen batteries. ACS Appl Energy Mater, 2019, 2: 4144–4150

13 Wang Y, Qiao M, Li Y, et al. Tuning surface electronic configuration of NiFe LDHs nanosheets by introducing cation vacancies (Fe or Ni) as highly efficient electrocatalysts for oxygen evolution reaction. Small, 2018, 14: 1800136

14 Huang L, Yang L, Guo S, et al. Influence of interlayer water molecules in Ni-based catalysts for oxygen evolution reaction. J Energy Chem, 2021, 53: 316–322

15 Sun Z, Yuan M, Shi K, et al. Engineering lithium ions embedded in NiFe layered double hydroxide lattices to activate laminated Ni^{2+} sites as high-efficiency oxygen evolution reaction catalysts. Chem Eur J, 2020, 26: 7244–7249

16 Lin L, Sun Z, Yao H, et al. Tuning surface lattice strain toward a Pt-skin $CoPt_x$ truncated octahedron for hydrogen evolution reaction. J Phys Chem C, 2019, 123: 29722–29728

17 Sun Z, Yuan M, Lin L, et al. Needle grass-like cobalt hydrogen phosphate on Ni foam as an effective and stable electrocatalyst for the oxygen

evolution reaction. Chem Commun, 2019, 55: 9729–9732

18 Lin L, Sun Z, Yuan M, et al. α-MoC_{1-x} quantum dots encapsulated in nitrogen-doped carbon for hydrogen evolution reaction at all pH values. ACS Sustain Chem Eng, 2019, 7: 9637–9645

19 Sun Z, Yuan M, Yang H, et al. 3D Porous amorphous γ-CrOOH on Ni foam as bifunctional electrocatalyst for overall water splitting. Inorg Chem, 2019, 58: 4014–4018

20 Sun Z, Lin L, Nan C, et al. Amorphous boron oxide coated NiCo layered double hydroxide nanoarrays for highly efficient oxygen evolution reaction. ACS Sustain Chem Eng, 2018, 6: 14257–14263

21 Gong M, Li Y, Wang H, et al. An advanced Ni-Fe layered double hydroxide electrocatalyst for water oxidation. J Am Chem Soc, 2013, 135: 8452–8455

22 Jia G, Hu Y, Qian Q, et al. Formation of hierarchical structure composed of (Co/Ni)Mn-LDH nanosheets on MWCNT backbones for efficient electrocatalytic water oxidation. ACS Appl Mater Interfaces, 2016, 8: 14527–14534

23 Chen D, Yan S, Chen H, et al. Hierarchical Ni-Mn layered double hydroxide grown on nitrogen-doped carbon foams as high-performance supercapacitor electrode. Electrochim Acta, 2018, 292: 374–382

24 Sun Z, Wang Y, Lin L, et al. Engineering borate modified NiFe layer double hydroxide nanoarrays as “hydroxyl ions hungry” electrocatalysts for enhanced oxygen evolution. Chem Commun, 2019, 55: 1334–1337

25 Bi Y, Cai Z, Zhou D, et al. Understanding the incorporating effect of Co^{2+}/Co^{3+} in NiFe-layered double hydroxide for electrocatalytic oxygen evolution reaction. J Catal, 2018, 358: 100–107

26 Liu D, Du Y, Li T, et al. One-step synthesis of IrO_x-decorated ultrathin NiFe LDH nanosheets for efficient oxygen evolution reaction. Chem Commun, 2020, 56: 11465–11468

27 Liang H, Meng F, Cabán-Acevedo M, et al. Hydrothermal continuous flow synthesis and exfoliation of NiCo layered double hydroxide nanosheets for enhanced oxygen evolution catalysis. Nano Lett, 2015, 15: 1421–1427

28 Jiang J, Zhang A, Li L, et al. Nickel-cobalt layered double hydroxide nanosheets as high-performance electrocatalyst for oxygen evolution reaction. J Power Sources, 2015, 278: 445–451

29 Leng X, Zeng Q, Wu K H, et al. Reduction-induced surface amorphization enhances the oxygen evolution activity in Co_3O_4. RSC Adv, 2015, 5: 27823–27828

30 Song F, Hu X. Ultrathin cobalt-manganese layered double hydroxide is an efficient oxygen evolution catalyst. J Am Chem Soc, 2014, 136: 16481–16484

31 Kim T W, Woo M A, Regis M, et al. Electrochemical synthesis of spinel type $ZnCo_2O_4$ electrodes for use as oxygen evolution reaction catalysts. J Phys Chem Lett, 2014, 5: 2370–2374

32 Xu Y, Wang Z, Tan L, et al. Fine tuning the heterostructured interfaces by topological transformation of layered double hydroxide nanosheets. Ind Eng Chem Res, 2018, 57: 10411–10420

33 Yang F, Zhao P, Hua X, et al. A cobalt-based hybrid electrocatalyst derived from a carbon nanotube inserted metal-organic framework for efficient water-splitting. J Mater Chem A, 2016, 4: 16057–16063

34 Peng W, Zheng G, Wang Y, et al. Zn doped ZIF67-derived porous carbon framework as efficient bifunctional electrocatalyst for water splitting. Int J Hydrog Energy, 2019, 44: 19782–19791

35 Wang S, Qin J, Meng T, et al. Metal-organic framework-induced construction of actiniae-like carbon nanotube assembly as advanced multifunctional electrocatalysts for overall water splitting and Zn-air batteries. Nano Energy, 2017, 39: 626–638

Summary for “用于高效电催化析氧反应的锰掺杂镍铁双金属氢氧化物催化剂”

Manganese-doped nickel-iron bimetallic hydroxide catalyst for efficient electrocatalytic oxygen evolution reaction

Zemin Sun[1,2], Yuhui Liu[1], Dajie Ding[1], Lanke Luo[1], Zhijie Li[1], Mengwei Yuan[1] & Genban Sun[1,2*]

[1] *Beijing Key Laboratory of Energy Conversion and Storage Materials Institution, College of Chemistry, Beijing Normal University, Beijing 100875, China;*
[2] *Center for Advanced Materials Research, Advanced Institute of Natural Sciences, Beijing Normal University at Zhuhai, Zhuhai 519087, China*
* Corresponding author, E-mail: gbsun@bnu.edu.cn

Hydrogen energy has many advantages such as wide source, high calorific value, clean and renewable energy, which is considered ideal secondary energy. Under the background of “carbon peak” and “carbon neutral”, the development of hydrogen energy has become the strategic deployment of all countries in the world. Renewable energy is converted into electric energy, and hydrogen production from water electrolysis is further realized through electric energy, which is currently considered as one of the safe and green way of hydrogen production. However, in the actual process of hydrogen production by electrolysis of water, there are problems such as high reaction overpotential and low energy conversion efficiency, which seriously restrict the cost of hydrogen production. During water electrolysis, hydrogen evolution reaction (HER) and oxygen evolution reaction (OER) occur at negative and positive electrodes respectively. Compared with the HER process of the two-electron reaction, the four-electron OER process requires a higher overpotential. Therefore, the four-electron OER process becomes the decisive step of the reaction. In order to achieve high efficiency and low energy consumption of hydrogen production process, it is urgent to use cheap, efficient and stable OER catalyst. At present, the search for efficient and low-cost OER catalyst is still the “holy grail” of water splitting. Among many non-noble metal catalysts, NiFe-layered double hydroxides (NiFe-LDHs) are considered as an ideal OER electrocatalyst in alkaline conditions due to their low raw material cost and adjustable structure. However, for NiFe-LDHs laminates, it is generally believed that the edge metal sites have higher catalytic activity than the internal metal sites, which leads to the insufficient utilization of the metal sites inside the laminates and reduces the catalytic activity of the OER reaction.

In order to solve the above problems, based on the microstructural regulation of NiFe-LDHs, some methods have been used to improve its catalytic activity and stability in the OER process. Heterogeneous element doping is considered to be an effective method to regulate the electronic structure and electrochemical activity of catalysts. Metal ion doping (Cr, Cu, V, etc.) can optimize the electronic structure of nickel metal active site, reduce reaction overpotential, and improve catalytic efficiency. However, the high biotoxicity of traditional transition metals (Cr, V, Cu, etc.) limits their industrial application. Mn ($Mn^{2+}\rightleftharpoons Mn^{3+}\rightleftharpoons Mn^{4+}$) with rich variation characteristics has a potential role in regulating lamellar charge characteristics.

Herein, in order to fully improve the utilization of NiFe-LDHs laminates, this study introduces manganese ions with variable valence characteristics into NiFe-LDHs laminates (Mn-NiFe-LDHs), and utilizes the variable valence characteristics of manganese ions to fully enhance the carrier mobility and promote electron transfer in the laminate. At the same time, due to the electronegativity characteristics of manganese ions, part of the electrons will be transferred from the vicinity of the nickel site to the vicinity of the manganese site, causing the nickel site to exhibit electron-deficient characteristics, which enhance the overall capture of the electron-rich oxygen-containing functional groups of the laminate, thereby effectively enhancing the OER catalytic activity. According to the results of the catalytic reaction, the Mn-NiFe-LDHs electrode exhibits an overpotential of only 332 mV at a current density of 10 mA/cm^2, which is lower than the initial NiFe-LDHs of 384 mV. The reasonable doping of manganese ions can effectively adjust the Ni^{2+} site activity and enhance its electrocatalytic activity. And to further clarify the effect of doping on the activity of LDHs laminates to provide experimental facts support.

electrochemistry, doping regulation, NiFe-layered double hydroxides, oxygen evolution reaction

doi: 10.1360/TB-2021-1323